Original Article

Insufficient radiofrequency ablation promotes the growth of non-small cell lung cancer cells through PI3K/Akt/HIF-1α signals

Jun Wan[1,†], Wei Wu[2,†], Yun Chen[1], Ningning Kang[1], and Renquan Zhang[1,*]

[1]Department of Thoracic Surgery, The First Affiliated Hospital of Anhui Medical University, Hefei 230022, China, and
[2]Department of Hematology, The First Affiliated Hospital of Anhui Medical University, Hefei 230022, China

[†]These authors contributed equally to this work.

*Correspondence address. Tel: +86-13966771605; Fax: +86-551-63633742; E-mail: zhangrqamu@163.com

Abstract

Accelerated progression of residual non-small cell lung cancer (NSCLC) after incomplete radiofrequency ablation (RFA) has frequently been reported. In this study, NSCLC cells A549, CCL-185, and H358 were treated using a water bath at 47°C for 5, 10, 15, 20, and 25 min gradually to establish the sublines A549-H, CCL-185-H, and H358-H, respectively. A549-H, CCL-185-H, and H358-H cells showed a significant increase in proliferation rate when compared with their corresponding parental cells *in vitro*. The expression of hypoxia-inducible factor-1α (HIF-1α) was obviously upregulated in both A549-H and CCL-185-H cells. Silencing of HIF-1α abolished the insufficient RFA-induced proliferation in A549-H and CCL-185-H cells. Furthermore, insufficient RFA treatment markedly elevated the phosphorylation of ERK1/2 and Akt, but not of p38 MAPK or JNK, in A549-H and CCL-185-H cells. The inhibitor of Akt, LY294002, but not the inhibitor of ERK1/2, PD98059, suppressed the upregulation of HIF-1α and the proliferation of A549-H and CCL-185-H cells *in vitro*. The *in vivo* results confirmed that insufficient RFA could trigger the tumor growth, upregulate the HIF-1α expression, and activate Akt in A549 xenograft tumors. Our data suggest that insufficient RFA can promote the *in vitro* and *in vivo* growth of NSCLC via upregulating HIF-1α through the PI3K/Akt signals.

Key words: insufficient RFA, NSCLC, proliferation, HIF-1α, PI3K/Akt

Introduction

Primary lung cancer is the most common cause of death due to cancer worldwide. Non-small cell lung cancer (NSCLC), which is one of the leading causes of cancer-related death, constitutes 80% of primary lung carcinoma [1]. Pneumonectomy or lobectomy with mediastinal lymph node sampling is the gold-standard treatment for early-stage NSCLC [2]. However, the high incidence of comorbidities and metastases often makes it technically not feasible for surgery. For example, it is estimated that >20% of patients with early-stage lung cancer did not undergo surgery [3]. Therefore, novel treatment approaches are needed for clinical NSCLC therapy.

Radiofrequency ablation (RFA), as a minimally invasive alternative therapy, has been considered as a potential curative for small primary lung tumors and lung metastases in patients who are medically inoperable [4,5]. In 2000, Dupuy *et al.* [6] reported the first three clinical cases of percutaneous lung RFA. Since then, RFA has been increasingly utilized as a nonsurgical treatment option for patients with primary and metastatic lung tumors [5,7,8]. RFA can locally heat the tumor to a lethal temperature while doing minimal damage to the surrounding normal lung tissue [9]. Furthermore, image-guided percutaneous RFA can reduce morbidity, mortality, cost, and hospital stay compared with those of open surgery.

One of the major problems for RFA is the difficulty in achieving complete tumor destruction [10]. This is because of the fact that the periphery of the tumor is distant from the center of ablation; therefore, the target temperature for ablation cannot be easily achieved

throughout the tumor [11]. Recently, more and more clinical cases about the rapid growth of residual cancer cells after RFA have been reported [12,13]. The mechanistic investigations suggested that RFA may alter tumor microenvironment to enhance the outgrowth of residual tumor cells or directly influence tumor cells to promote progression of residual tumor [12,14,15]. Insufficient RFA will also lead to activation of various downstream signaling molecules such as MAPK and PI3K/Akt [12,16], which can trigger the proliferation of cancer cells. However, most of these results and conclusions are based on the hepatocellular carcinoma. The effects of insufficient RFA on the progression of lung cancer, particularly for NSCLC, and the mechanisms involved in the process have not been clearly determined.

In the present study, we investigated the effects and mechanisms of insufficient RFA on the progression of NSCLC cells both *in vitro* and *in vivo*. Our results revealed that insufficient RFA can trigger the proliferation of NSCLC cells via PI3K/Akt/HIF-1α signals. The *in vivo* results confirmed that insufficient RFA can trigger the growth, upregulate the HIF-1α, and activate Akt in A549 xenograft tumors.

Materials and Methods

Chemicals and reagents

All chemicals were of reagent grade or better and were purchased from Sigma Chemical Co. (St Louis, USA) unless otherwise noted. PD 98059 (MAPK/ERK inhibitor), LY294002 (PI3K/Akt inhibitor), and YC-1 (HIF-1α inhibitor) were purchased from Beyotime (Nanjing, China). Antibodies against Bcl-2, PCNA, HIF-1α, Akt, p-Akt, ERK1/2, p-ERK1/2, p38 MAPK, p-p38 MAPK, JNK, p-JNK and GAPDH, and horseradish peroxidase (HRP)-conjugated secondary antibody were purchased from Cell Signaling Technology (Beverly, USA). PrimeScript® RT reagent kit and SYBR® Premix Ex Taq™ were products of TaKaRa (Dalian, China). E.Z.N.A® HP Total RNA kit was obtained from Omega Bio-Tek (Doraville, USA).

Cell culture

Human NSCLC cell lines A549, CCL-185, and H358 were purchased from the American Type Culture Collection (ATCC, Manassas, USA) and maintained in high-glucose Dulbecco's modified Eagle medium (DMEM) supplemented with 10% fetal bovine serum, 100 U/ml penicillin, and 100 µg/ml streptomycin (Life Technologies, Cergy Pontoise, France) in a humidified atmosphere of 5% CO_2 at 37°C.

Insufficient RFA treatment

The *in vitro* insufficient RFA treatment was conducted as previously described [12,17]. Briefly, A549, CCL-185, or H358 cells were seeded into the 6-well plates, cultured for 24 h, sealed, and submerged in a water bath set to 47°C for 5 min. Cells were allowed to recover to 80% confluence, and then exposed to above heat treatment for 10 min. Then the process was repeated and cells were sequentially exposed to above heat treatment for 15, 20, and 25 min. Cells survived from the treatment were designated as A549-H, CCL-185-H, and H358-H, respectively.

Cell viability assay

The cell viability was evaluated by 3-(4, 5-dimethylthiazol-2-yl)-2, 5-diphenyltetrazolium bromide (MTT) assay according to the previous study [18]. Cells were seeded at a concentration of 2×10^3/well in 96-well plates. MTT solution was added to each well at a final concentration of 0.5 mg/ml and incubated for 4 h. At the end of incubation, formazan crystals resulting from MTT reduction were dissolved by addition of 150 µl dimethyl sulfoxide per well. The optical density was measured at 570 nm with a microplate reader (model 550, BioRad, Hercules, USA).

Western blot analysis

The A549-H, CCL-185-H, or H358-H cells and their parental cells were lysed in cell lysis buffer, and then the lysates were cleared by centrifugation and denatured by boiling in Laemmli buffer. Aliquots of protein were separated on 10% sodium dodecyl sulfate–polyacrylamide gels and electrophoretically transferred to nitrocellulose membranes. After being blocked with 5% nonfat milk at room temperature for 2 h, membranes were incubated with the primary antibody at 1:1000 dilution overnight at 4°C and then incubated with an HRP-conjugated secondary antibody at 1:1000 dilution for 2 h at room temperature, and finally detected with the Western Lightning Chemiluminescent detection reagent (Perkin-Elmer Life Sciences, Wellesley, USA).

Real-time polymerase chain reaction assay

Total mRNA was extracted using the TRIzol reagent (Invitrogen, Carlsbad, USA), and reverse transcription was performed using an RT-PCR kit. Real-time experiments were conducted on a DNA Engine Opticon System (MJ Research Inc., Guilford, USA) using SYBR Green PCR Master Mix kit and specific primers. The sequences of primers to determine the expression of the target gene were listed as follows: *GAPDH*, forward: 5′-GCACCGTCAAGGCTGAGAAC-3′ and reverse: 5′-TGGTGAAGACGCCAGTGGA-3′; HIF-1α, forward: 5′-GCGGCA TGAATCTATTGGAC-3′ and reverse 5′-CCCAGGAAGCCGTCTTTA TT-3′. Comparative threshold cycle (CT) values were reported relative to *GAPDH* mRNA. The cycle number when the fluorescence first reached a preset threshold (C_t) was used to quantify the initial concentration of individual templates for expression of mRNA of genes of interest. All experiments were performed three times independently and the average was used for comparison.

Transient transfection of small-interfering RNAs

To further examine the functional role of HIF-1α in A549-H and CCL-185-H cells, transient transfection was performed in cells with small-interfering RNA (siRNA) targeting *HIF-1α* mRNA (siCTTNB1, Gene Parma, Shanghai, China) or mock transfection (Gene Parma). Cells were transfected with either a control or an siRNA using Lipofectamine 2000 (Invitrogen) in OPRI-MEM medium (Gibco, Gaithersburg, USA) according to the manufacturer's instructions. The sequence of HIF-1α siRNA was 5′-CCACCACUGAUGAAUUAAATT-3′.

Xenograft assays

Male BALB/c nude mice (5 weeks old) were randomized into four groups and housed in laminal-flow cabinets under specific pathogen-free conditions. Then 2×10^6 cell A549-H ($n = 18$) or parental A549 cells ($n = 6$) were suspended in 200 µl serum-free DMEM and matrigel (1 : 1), and then injected subcutaneously into the upper right flank region of nude mice. After establishment, A549-H tumor-bearing mice were treated with YC-1 (HIF-1α inhibitor, $n = 6$) or LY294002 (PI3K/Akt inhibitor, $n = 6$) (5 mg/kg i.p. qd) for every 3 days. Tumor size was measured with a caliper rule for every 3 days. The tumor volume was estimated with the formula '$a \times b^2 \times 0.5$', in which a represents the longest and b represents the shortest radius of the tumor in

millimeters. At the end of the experiments, mice were euthanized, and tumor tissues were removed and fixed for histological examination and immunohistochemical staining.

Immunohistochemistry

Immunohistochemistry staining of formalin-fixed paraffin-embedded tissue was conducted as previously described [19]. Briefly, tumor tissues were fixed in formalin and embedded in paraffin. Sections (5 μm) were deparaffinized and hydrated, and endogenous peroxidase activity was blocked with 3% H_2O_2 in water for 10 min. Antigen retrieval was done with 10 mM citrate buffer (pH 6.0) for 10 min. Slides were incubated with Biocare blocking reagent for 10 min to block non-specific binding. Then, they were incubated with p-Akt or HIF-1α antibody overnight at 4°C. Slides were washed with phosphate buffered saline (PBS) twice and then incubated with goat anti-rabbit HRP-conjugated secondary antibodies for 30 min at room temperature and then washed. Finally, slides were incubated with 3,3′-diaminobenzidine and counter stained with hematoxylin.

Statistical analysis

All values were expressed as the mean ± SD. The data were analyzed using Student's t test or the analysis of variance test. $P < 0.05$ was considered statistically significant. GraphPad Prism (GraphPad Software Inc., San Diego, USA) was used for these analyses.

Results

Insufficient RFA treatment promotes the proliferation of NSCLC cells *in vitro*

In order to evaluate the effects of insufficient RFA treatment, we measured the cell viability of A549-H, CCL-185-H, and H358-H cells and compared with their corresponding parental cells. The MTT assays showed that A549-H had significant ($P < 0.05$) greater cell viability when compared with A549 cells at 24, 48, and 72 h (**Fig. 1A**). Similarly,

the cell viability of CCL-185-H (**Fig. 1B**) and H358-H (**Fig. 1C**) cells were also significantly ($P < 0.05$) greater than that of their corresponding parental cells. The proliferation rates of A549-H, CCL-185-H, and H358-H were ~2.8, 2.0, and 1.4 folds of their corresponding parental cells at 72 h, respectively. To further verify the role of insufficient RFA in cell viability of NSCLC cells, the expression of Bcl-2 and PCNA, markers of cell viability, were detected by western blot analysis. The results showed that A549-H cells had obviously greater expression of Bcl-2 and PCNA than A549 cells. Similar phenomenon was also observed in CCL-185-H and H358-H cells (**Fig. 1D**). Collectively, our data suggested that insufficient RFA treatment can significantly promote the growth of NSCLC cells *in vitro*.

Upregulation of HIF-1α mediates insufficient RFA-induced proliferation of NSCLC cells

Recent studies indicated that insufficient RFA treatment can increase the expression of HIF-1α in cancer cells [12,17] and then promote the invasion and angiogenesis. To verify the mechanisms for insufficient RFA-induced proliferation of NSCLC cells, we checked the mRNA and protein expression of HIF-1α. The results showed that the mRNA and protein expression of HIF-1α in A549-H cells were obviously greater than that in A549 cells. Similar elevated expression of HIF-1α was also observed in CCL-185-H cells (**Fig. 2A,B**). To verify the role of HIF-1α in insufficient RFA-induced proliferation of NSCLC cells, we knocked down its expression by the use of siRNA (**Fig. 2C**). Interestingly, the knockdown of HIF-1α significantly attenuated the insufficient RFA-induced proliferation of A549-H and CCL-185-H cells (**Fig. 2D**). These results suggested that upregulation of HIF-1α may mediate insufficient RFA-induced proliferation of NSCLC cells.

Insufficient RFA modulates the activities of MPAK and PI3K/Akt signals

Previous studies indicated that insufficient RFA will lead to the activation of various downstream signaling molecules such as MAPK and
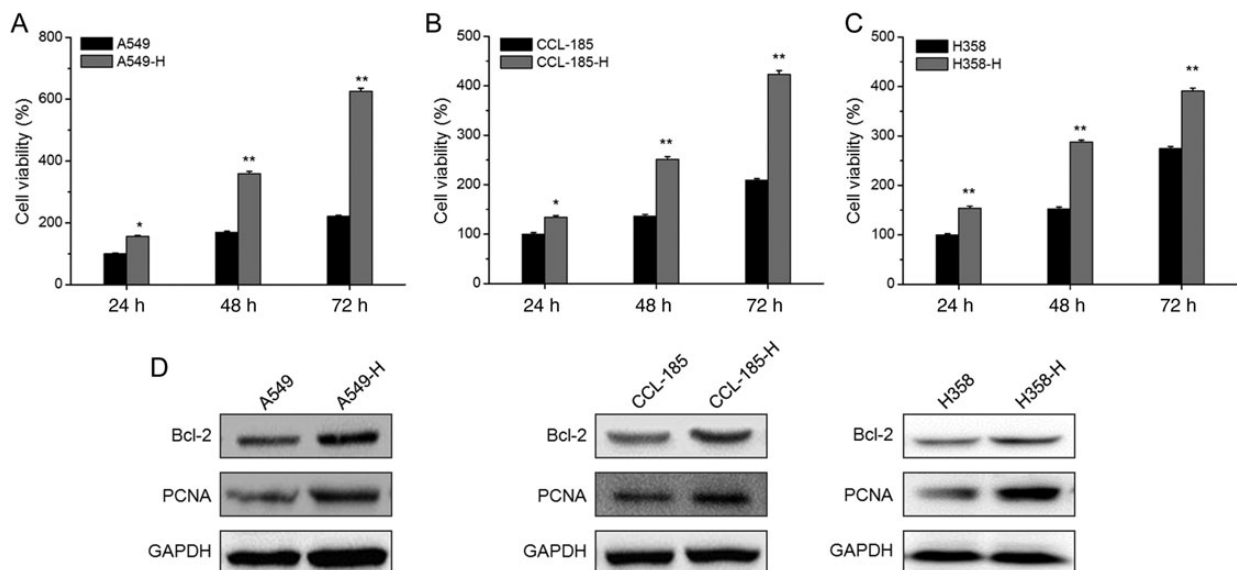

Figure 1. Insufficient RFA treatment promotes the proliferation of NSCLC cells *in vitro* The A549-H (A), CCL-185-H (B), and H358-H (C) cells and their corresponding parental cells were cultured for 24, 48, and 72 h, and then cell viability was assessed by MTT assay. (C) The protein expression of Bcl-2 and PCNA in A549-H, CCL-185-H, and H358-H cells and their corresponding parental cells were measured by western blot analysis. Data are presented as means ± SD of six independent experiments. *$P < 0.05$ compared with control; **$P < 0.01$ compared with control.
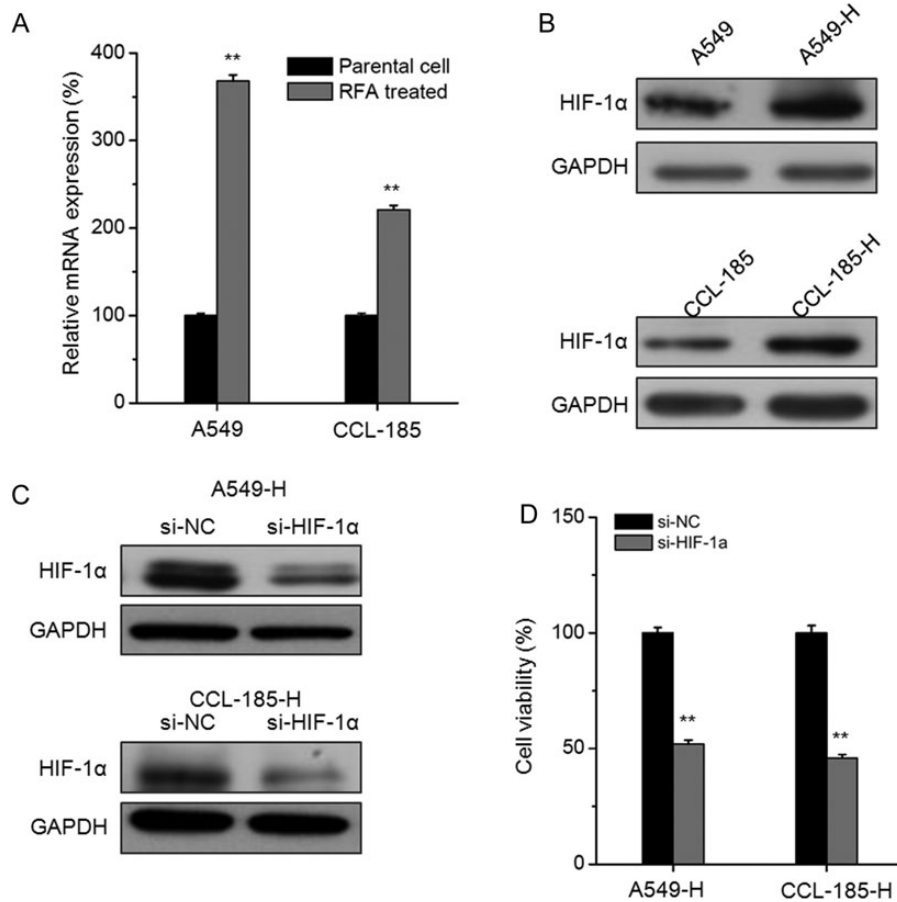
Figure 2. The upregulation of HIF-1α mediates insufficient RFA-induced proliferation of NSCLC cells The mRNA (A) and protein (B) levels of HIF-1α in A549-H and CCL-185-H cells and their corresponding parental cells were measured by real-time polymerase chain reaction and western blot analysis, respectively. **$P < 0.01$ compared with the parental cell. (C) Cells were transfected with si-NC or si-HIF-1α for 24 h, then the expression of HIF-1α was measured. (D) A549-H and CCL-185-H cells were transfected with si-NC or si-HIF-1α for 48 h, and the cell viability was detected by MTT assay. Data are presented as means ± SD of six independent experiments. **$P < 0.01$ compared with si-NC.

PI3K/Akt [12,16]. Therefore, the effects of insufficient RFA treatment on the activation of MAPK and PI3K/Akt were investigated. As shown in **Fig. 3A**, there was obviously increased phosphorylation of Akt and ERK1/2 in A549-H cells, but not of p38 MAPK and JNK. Similarly, the increased phosphorylation of Akt and ERK1/2 was also observed in CCL-185-H cells (**Fig. 3B**). These data suggested that insufficient RFA treatment can activate Akt and ERK1/2 in NSCLC cells.

PI3K/Akt mediates insufficient RFA-induced HIF-1α upregulation and cell proliferation

To investigate whether the activation of ERK1/2 and PI3K/Akt participates in insufficient RFA-induced HIF-1α upregulation and cell proliferation, the PI3K/Akt inhibitor LY294002 and ERK inhibitor PD98059 were used according to previous studies [20]. As shown in **Fig. 4A**, PI3K/Akt inhibitor LY294002, but not ERK inhibitor PD98059, could significantly abolish the upregulation of HIF-1α in A549-H (**Fig. 4A**) and CCL-185-H (**Fig. 4B**) cells. These results suggested that PI3K/Akt, but not ERK1/2, mediated the insufficient RFA-induced upregulation of HIF-1α in NSCLC cells. Furthermore, A549-H and CCL-185-H cells were treated with LY294002 and PD98059 for 24 h, and then the cell vitality was measured by MTT assay. The results revealed that LY294002, rather than PD98059, significantly inhibited the *in vitro* proliferation of A549-H and

CCL-185-H cells (**Fig. 4C**). These data revealed that PI3K/Akt mediates insufficient RFA-induced HIF-1α upregulation and proliferation of NSCLC cells.

PI3K/Akt/HIF-1α signals mediate insufficient RFA-induced growth of NSCLC cells *in vivo*

We further examined the growth of the A549 tumor and A549-H tumor, and the effects of LY294002 and YC-1 on the growth of tumor xenografts in nude mice. Ten days after the injection, A549-H cells began to form measurable tumors, the volume of which increased with time (**Fig. 5A**). However, A549 cells produced measurable tumors only after 16–19 days. After 34 days, all mice were sacrificed due to the large volume of tumor in the A549-H group. During the experiments, the average size of tumor in A549-H groups was significantly ($P < 0.05$) greater than that of A549 groups (**Fig. 5A**). In addition, both LY294002 and YC-1 treatment significantly ($P < 0.05$) diminished the difference of the tumor growth between A549-H tumor and parental A549 tumor, and the inhibitory effects of LY294002 and YC-1 were not significantly ($P > 0.05$) different (**Fig. 5A**). Similarly, the volumes of the A549-H tumor xenografts were significantly ($P < 0.05$) higher than those of the parental A549 tumor. Additionally, the volumes of groups injected with LY294002 or YC-1 were markedly decreased in comparison with that of A549-H groups (**Fig. 5B**).
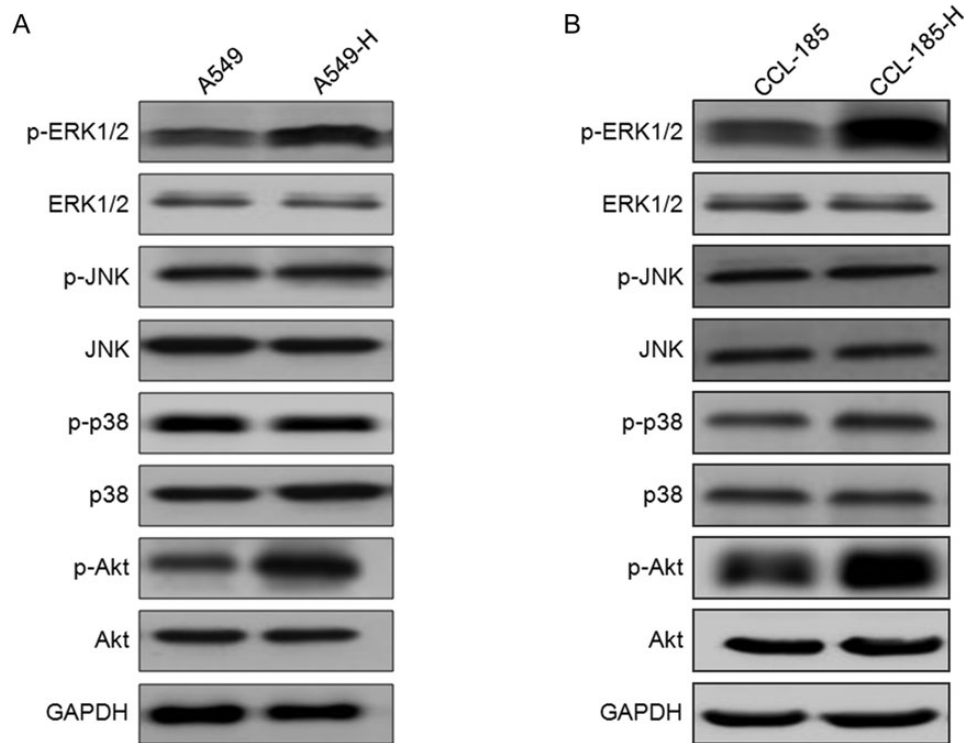
Figure 3. The variation of MAPK and PI3K/Akt in NSCLC cells treated by insufficient RFA   The phosphorylation and total ERK1/2, JNK, p38 MAPK, and Akt were detected in A549-H (A) and CCL-185-H (B) cells by western blot analysis and compared with their corresponding parental cells.
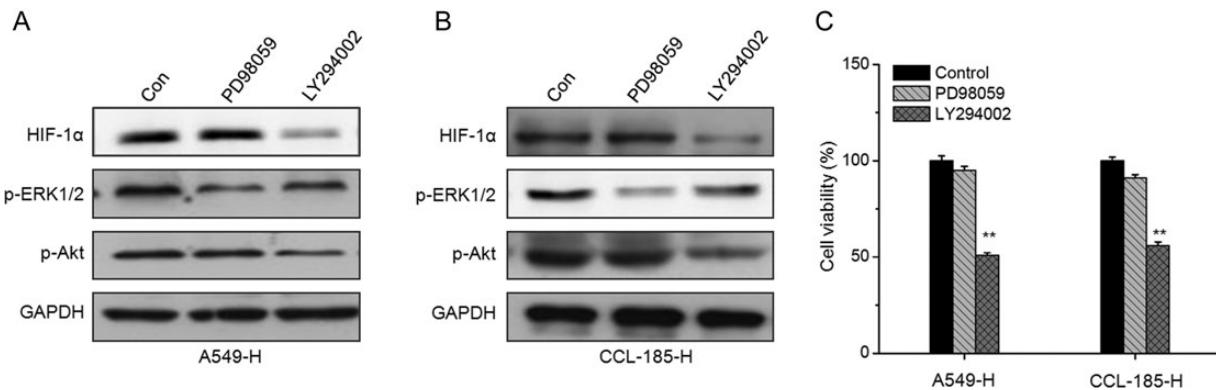

Figure 4. PI3K/Akt mediates insufficient RFA-induced HIF-1α upregulation and cell proliferation   A549-H (A) and CCL-185-H (B) cells were treated with PD98059 (10 μM) or LY294002 (10 μM) for 24 h, and then the expression of HIF-1α, p-ERK1/2, and p-Akt was examined by western blot analysis. (C) A549-H or CCL-185-H cells were treated with PD98059 (10 μM) or LY294002 (10 μM) for 24 h, and then cell viability was measured by MTT assay. Data are presented as means ± SD of three independent experiments. **$P < 0.01$ compared with control.

Western blot analysis showed that the expression of HIF-1α and Akt was obviously higher in the A549-H group than that in parental A549 tumor (**Fig. 5C**). LY294002 significantly inhibited the expression of Akt and HIF-1α in the A549-H group. Furthermore, YC-1 significantly suppressed the expression of HIF-1α, but not of Akt, in the A549-H group. This was further confirmed by the results of immunohistochemical study (**Fig. 5D**). These data suggested that PI3K/Akt/HIF-1 signals mediate insufficient RFA-induced growth of NSCLC cells *in vivo*.

Discussion

RFA is safe and effective for lung cancer therapy. However, the phenomenon of rapid growth of residual lung tumor after RFA has been observed in many clinical centers, while the detailed mechanisms have not been well illustrated. The illustration of biological behaviors of residual NSCLC and the mechanisms involved are important to improve the prognosis of NSCLC patients. In the present study, we revealed that insufficient RFA can significantly promote the *in vitro* proliferation of NSCLC cells. HIF-1α was markedly elevated during this process, while silence of HIF-1α alleviated insufficient RFA-induced cell proliferation. Insufficient RFA can activate ERK1/2 and Akt in NSCLC cells. Inhibition of PI3K/Akt, but not of ERK1/2, attenuated insufficient RFA-induced HIF-1α upregulation and cell proliferation. The results of *in vivo* xenografts also confirmed that insufficient RFA can trigger the growth of NSCLC, while inhibitor of PI3K/Akt or HIF-1α can attenuate this effect. Collectively, our results revealed
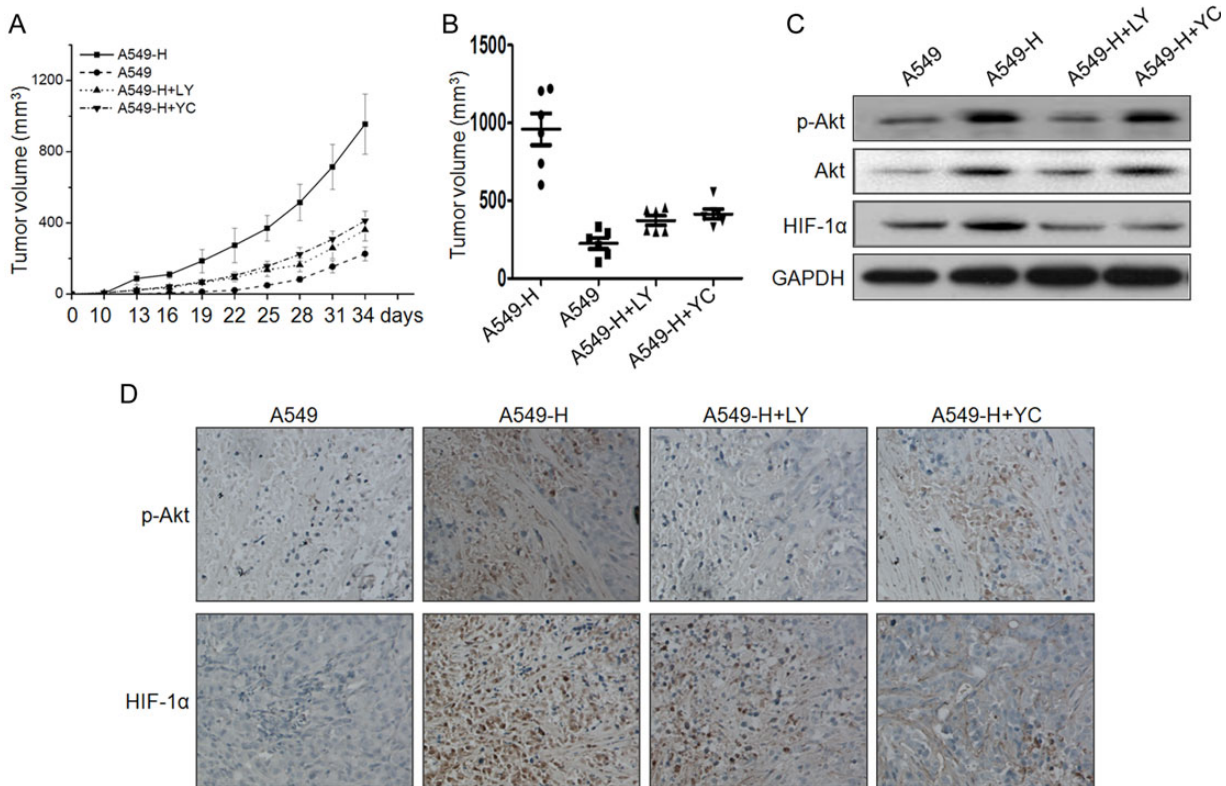
Figure 5. PI3K/Akt/HIF-1α signals mediate insufficient RFA-induced *in vivo* growth of NSCLC cells (A) Average tumor volume is shown for the A549 tumors. Parental A549 tumors with PBS (*n* = 6), A549-H tumors with PBS (*n* = 6), and A549-H tumors with LY (LY294002, *n* = 6) or YC (YC-1, *n* = 6). (B) Mice were killed 34 days after implantation and the tumor tissues were removed and measured. (C) The protein levels of p-Akt, Akt, and HIF-1α were determined by western blot analysis in the tumor lysates. (D) The tumor tissue sections of each group were subjected to immunohistochemistry detection of p-Akt and HIF-1α.

that insufficient RFA can facilitate the progression of NSCLC cells by promoting the *in vitro* and *in vivo* growth via PI3K/Akt/HIF-1α signals.

RFA induces coagulation necrosis once the tissue temperature exceeds 50°C for 4–6 min [21]. Recent studies suggested that if cancer cells are not completely coagulated, the residual tumor cells are prone to proliferation, invasion, and angiogenesis [12,13]. This is also observed in our present study that the proliferation rates of A549-H, CCL-185-H, and H358-H were ~2.8, 2.0, and 1.4 folds of their corresponding parental cells, respectively. Our data are consistent with the results that one of HepG2 sublines showed >100% increase in proliferation, marked heat tolerance, and no obvious difference in invasiveness compared with parental HepG2 cells [17]. Another study demonstrated that one subline of HepG2 cells showed 18.8% ± 3.1% increase in cell viability compared with parental HepG2 cells [12]. The difference might be due to the variation of cell lines and insufficient RFA treatment.

HIF-1α, a component of HIF-1, can promote the progression of various cancer cells via facilitating the cell proliferation, metastasis, and tumor angiogenesis [22,23]. RFA has been reported to trigger the angiogenesis and proliferation of residual hepatocellular carcinoma via upregulation of HIF-1α [12,24]. Hyperthermia may play an important role in the rapid growth of residual cancer cells after RFA by promoting angiogenesis via HIF-1α/VEGFA [12]. Our present study revealed that the mRNA and protein levels of HIF-1α were significantly increased in insufficient RFA-treated NSCLC cells when compared with their parental cells. Furthermore, silence of HIF-1α attenuated

insufficient RFA-induced cell proliferation. This result confirmed that HIF-1α plays an essential role in insufficient RFA-induced progression of NSCLC.

Previous studies suggested that HIF-1α is regulated by several upstream cellular signals including RAS/MARK, PI3K/Akt/mTOR, succinate dehydrogenase, and reactive oxygen species [25,26]. Therefore, we investigated the underlying molecular mechanisms responsible for the upregulation of HIF-1α in insufficient RFA-treated NSCLC cells. The results showed that the elevated phosphorylation of Akt and ERK1/2, but not of p38 MAPK or JNK, was observed in A549-H and CCL-185-H cells. In addition, the inhibitor of Akt, but not of ERK1/2, suppressed the upregulation of HIF-1α and increased proliferation of A549-H and CCL-185-H cells. These data suggested that insufficient RFA can upregulate HIF-1α via PI3K/Akt signals in NSLCL cells, which has not been reported previously.

We also confirmed that insufficient RFA treatment can trigger the *in vivo* initiation and progression of NSCLC cells in xenograft mouse model. Both LY294002 and YC-1 can attenuate the *in vivo* growth of A549-H cells. Moreover, insufficient RFA also increased the expression of p-Akt, Akt, and HIF-1α in A549-H tumor. Based on the above findings, we postulated that the hyperthermia-induced NSCLC subline exerted its stronger growth effect through enhanced PI3K/Akt/HIF-1α signaling pathway. These novel findings could be a potential mechanism associated with the rapid growth of the residual tumor after RFA and, therefore, could have important therapeutic implications. Nevertheless, further studies are still needed to clarify the rapid growth of residual NSCLC cells after insufficient RFA treatment.

Funding

References

1. Reck M, Popat S, Reinmuth N, De Ruysscher D, Kerr KM, Peters S. Metastatic non-small-cell lung cancer (NSCLC): ESMO Clinical Practice Guidelines for diagnosis, treatment and follow-up. *Ann Oncol* 2014, 25: iii27–iii39.

2. Dienemann H. Principles of surgical treatment in localized non-small cell lung cancer. *Lung Cancer* 2001, 33(Suppl 1): S3–S8.

3. Bach PB, Cramer LD, Warren JL, Begg CB. Racial differences in the treatment of early-stage lung cancer. *N Engl J Med* 1999, 341: 1198–1205.

4. Zhu JC, Yan TD, Morris DL. A systematic review of radiofrequency ablation for lung tumors. *Ann Surg Oncol* 2008, 15: 1765–1774.

5. Gadaleta C, Catino A, Mattioli V. Radiofrequency thermal ablation in the treatment of lung malignancies. *In Vivo* 2006, 20: 765–767.

6. Dupuy DE, Zagoria RJ, Akerley W, Mayo-Smith WW, Kavanagh PV, Safran H. Percutaneous radiofrequency ablation of malignancies in the lung. *Am J Roentgenol* 2000, 174: 57–59.

7. Nguyen CL, Scott WJ, Goldberg M. Radiofrequency ablation of lung malignancies. *Ann Thorac Surg* 2006, 82: 365–371.

8. Yan TD, King J, Sjarif A, Glenn D, Steinke K, Morris DL. Learning curve for percutaneous radiofrequency ablation of pulmonary metastases from colorectal carcinoma: a prospective study of 70 consecutive cases. *Ann Surg Oncol* 2006, 13: 1588–1595.

9. Dupuy DE. Image-guided thermal ablation of lung malignancies. *Radiology* 2011, 260: 633–655.

10. Nijkamp MW, van der Bilt JD, de Bruijn MT, Molenaar IQ, Voest EE, van Diest PJ, Kranenburg O, et al. Accelerated perinecrotic outgrowth of colorectal liver metastases following radiofrequency ablation is a hypoxia-driven phenomenon. *Ann Surg* 2009, 249: 814–823.

11. Feng K, Yan J, Li X, Xia F, Ma K, Wang S, Bie P, et al. A randomized controlled trial of radiofrequency ablation and surgical resection in the treatment of small hepatocellular carcinoma. *J Hepatol* 2012, 57: 794–802.

12. Kong J, Pan B, Ke S, Dong S, Li X, Zhou A, Zheng L, et al. Insufficient radiofrequency ablation promotes angiogenesis of residual hepatocellular carcinoma via HIF-1alpha/VEGFA. *PLoS One* 2012, 7: e37266.

13. Ke S, Ding XM, Kong J, Gao J, Wang SH, Cheng Y, Sun WB. Low temperature of radiofrequency ablation at the target sites can facilitate rapid progression of residual hepatic VX2 carcinoma. *J Transl Med* 2010, 8: 73.

14. Nikfarjam M, Muralidharan V, Christophi C. Altered growth patterns of colorectal liver metastases after thermal ablation. *Surgery* 2006, 139: 73–81.

15. Kong J, Kong L, Ke S, Gao J, Ding X, Zheng L, Sun H, et al. After insufficient radiofrequency ablation, tumor-associated endothelial cells exhibit enhanced angiogenesis and promote invasiveness of residual hepatocellular carcinoma. *J Transl Med* 2012, 10: 230.

16. Dong S, Kong J, Kong F, Gao J, Ke S, Wang S, Ding X, et al. Insufficient radiofrequency ablation promotes epithelial-mesenchymal transition of hepatocellular carcinoma cells through Akt and ERK signaling pathways. *J Transl Med* 2013, 11: 273.

17. Matsumoto N, Ozawa S, Okamoto M, Ikeda H, Takahashi H, Matsunaga K, Okuse C, et al. Insufficient radiofrequency ablation therapy may induce further malignant transformation of hepatocellular carcinoma. *Hepatology* 2010, 52: 953a.

18. Ge LC, Chen ZJ, Liu H, Zhang KS, Su Q, Ma XY, Huang HB, et al. Signaling related with biphasic effects of bisphenol A (BPA) on Sertoli cell proliferation: a comparative proteomic analysis. *Biochim Biophys Acta* 2014, 1840: 2663–2673.

19. Liu H, Zhou BH, Qiu X, Wang HS, Zhang F, Fang R, Wang XF, et al. T63, a new 4-arylidene curcumin analogue, induces cell cycle arrest and apoptosis through activation of the reactive oxygen species-FOXO3a pathway in lung cancer cells. *Free Radic Biol Med* 2012, 53: 2204–2217.

20. Secchiero P, Gonelli A, Carnevale E, Milani D, Pandolfi A, Zella D, Zauli G. TRAIL promotes the survival and proliferation of primary human vascular endothelial cells by activating the Akt and ERK pathways. *Circulation* 2003, 107: 2250–2256.

21. Lencioni R. Loco-regional treatment of hepatocellular carcinoma. *Hepatology* 2010, 52: 762–773.

22. Carmeliet P, Dor Y, Herbert JM, Fukumura D, Brusselmans K, Dewerchin M, Neeman M, et al. Role of HIF-1alpha in hypoxia-mediated apoptosis, cell proliferation and tumour angiogenesis. *Nature* 1998, 394: 485–490.

23. Tang N, Wang L, Esko J, Giordano FJ, Huang Y, Gerber HP, Ferrara N, et al. Loss of HIF-1alpha in endothelial cells disrupts a hypoxia-driven VEGF autocrine loop necessary for tumorigenesis. *Cancer Cell* 2004, 6: 485–495.

24. Gwak GY, Yoon JH, Kim KM, Lee HS, Chung JW, Gores GJ. Hypoxia stimulates proliferation of human hepatoma cells through the induction of hexokinase II expression. *J Hepatol* 2005, 42: 358–364.

25. Harris AL. Hypoxia—a key regulatory factor in tumour growth. *Nat Rev Cancer* 2002, 2: 38–47.

26. Hu YZ, Liu J, Huang H. Recent agents targeting HIF-1 alpha for cancer therapy. *J Cell Biochem* 2013, 114: 498–509.